Run Group B Proposal: Quasi-real Photoproduction on Deuterium

Florian Hauenstein (Spokesperson), Mohammad Hattawy, and Lawrence Weinstein

Old Dominion University, Norfolk, Virginia 23529

William Phelps (Co-spokesperson), Izzy Illari, William Briscoe, Igor Strakovsky, Chan Kim, and Olga Cortez

The George Washington University, Washington D.C. 20052

Stepan Stepanyan (Co-spokesperson), Valery Kubarovsky, and Daniel Carman

Thomas Jefferson National Accelerator Facility, Newport News, Virginia 23606

Reynier Cruz-Torres, Efrain Segarra, and Axel Schmidt

Massachusetts Institute of Technology, Cambridge, Massachusetts 02139

Yordanka Ilieva

University of South Carolina, Columbia, South Carolina 29201

Bryan McKinnon

University of Glasgow, Glasgow G12 8QQ, UK

Lei Guo

Florida International University, Miami, Florida 33199

Raffaella de Vita, Andrea Celentano, and Marco Battaglieri

Istituto Nazionale Fisica Nucleare sezione di Genova, 16146 Genova GE, Italy

Carlos Salgado

Norfolk State University, Norfolk, Virginia 23504

Kenneth Hicks

University of Ohio, Athens, Ohio 45701

John Price

California State University Dominguez Hills, Carson, California 90747

Silvia Niccolai

Institut de Physique Nuclaire d'Orsay, 91406 Orsay, France

(Dated: June 7, 2019)

CONTENTS

I. INTRODUCTION

The phenomenology of hadrons, and in particular the study of their spectrum, led more than forty years ago to the development of the quark model, where baryons and mesons are described as bound systems of three quarks and of a quark-antiquark pair, respectively. There are also predictions for baryon-baryon or baryon-antibaryon states or resonances [1–3]. The simplest baryon-antibaryon state is $p\bar{p}$ where some experiments reported the observation of narrow resonances [4–6]. However, none of these are unanimously measured. Furthermore, such resonances might be particularly non-conventional states, e.g., molecular states or glueballs.

We present a CLAS12 run-group B (RG-B) proposal to study the quasireal $p\bar{p}$ photoproduction off a neutron, as well as the coherent process off a deuteron to look for resonances in the $p\bar{p}$ invariant mass spectrum. Furthermore, the production mechanism of the $p\bar{p}$ will be investigated by studying the coherent production off deuteron of other dihadron pairs, namely $\pi^+\pi^-$ and K^+K^-.

A deuterium target will be used as an effective neutron target. The quasi-real photons will be produced by the incident electron beam in the target. We will collect data with tagged and untagged photos and will determine the invariant dihadron spectra ($d\sigma/dm$) as well as the t-dependence of the cross section ($d\sigma/dt$) .

The data will be taken during the remaining of the approved RG-B beam time, i.e., 69 PAC days. We are requesting a two-particle opposite-sector, opposite-charge trigger in the Forward Detector of CLAS12 for the remaining RG-B beam time. This corresponds to the dimuon trigger used for J/ψ production, but without a cut on the energy deposition in the electromagnetic calorimeter of CLAS12. The conditions for beam energy, current, and polarization are the same as for the other RG-B experiments. The experimental setup needs CLAS12 and the Forward Tagger.

The proposal is organized as follows. In Section 2 we give a short motivation about the experiment and an overview of previous measurements of $p\bar{p}$ resonances. In Section 3 we describe the proposed measurement and the details of the experimental setup. The trigger and the expected photon luminosities are discussed in Section 4. The estimations of rates, and the studies of expected angular and t distributions for the reactions are shown in Section 5. Finally, a summary is given in Section 6.

II. MOTIVATION

Hadron spectroscopy plays an important role in hadron physics in particular for understanding the mechanism of confinement. While much progress has been made in understanding perturbative phenomena in QCD, the non-perturbative regime, the regime of hadrons, has remained largely difficult to calculate. There is a discrepancy between model predicted and experimentally observed baryon and meson states. Over the last decades significant efforts have been dedicate to investigate the spectrum of mesons and baryons. The research has been focused on unconventional or exotic states such as hybrids, glueballs or tetraquarks and highly excited $q\bar{q}$ states, which are either poorly established or not observed at all.

One of the interesting channels to look for non-conventional states is the proton-antiproton system. This channel has been studied for many years, using hadronic and electromagnetic probes. Some experiments reported evidences for resonance states which could be interpreted as mesons or molecule-like baryonium states. However, up to date there has not been a clear, high statistics proof of any of the reported states. The debate on the existence of these states has greatly lingered due to a lack of statistics, supporting evidence, and conflicting experimental results. This proposal aims to study the photoproduction of the proton-antiproton system on a neutron and coherently on the deuteron to provide the largest data set for these reactions and to search for $p\bar{p}$ resonances.

A study of the cross sections of coherent production of $p\bar{p}$ and meson pairs, $\pi^+\pi^-$ and K^+K^-, help allow to understand the underlying production mechanism. For example there have been speculations that baryon-antibaryon production in two-photon interactions proceeds via di-quark pair, (qq) and $(\bar{q}\bar{q})$, instead of $(q\bar{q})$ [7].

A. $p\bar{p}$ Resonances

1. *Previous Measurements*

The $p\bar{p}$ spectrum has been studied for many years, using hadronic and electromagnetic probes. One of the first observations of a resonance decaying into a $p\bar{p}$ pair was in the reaction $\pi^- p \to \pi^- p_{\text{fast}} p\bar{p}$ [4]. The experiment was performed at the CERN' Omega spectrometer. Two narrow peaks, one at $2.020\,\text{GeV}/c^2$ and $2.200\,\text{GeV}/c^2$, were seen, each with a width of about $20\,\text{MeV}/c^2$. There were other experiments which either confirmed [5] or refuted [8]

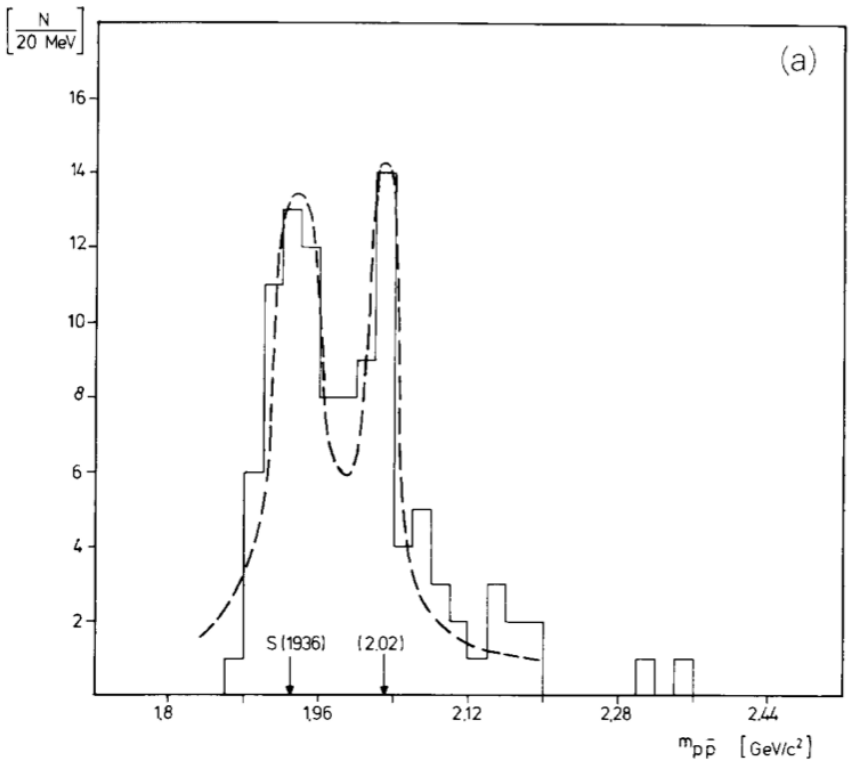

FIG. 1: The invariant mass distributions for $p\bar{p}$ in the photoproduction reaction $\gamma p \to pp\bar{p}$ from [9]. This distribution suggests two possible resonances at $1.936\,\mathrm{GeV}/c^2$ and $2.02\,\mathrm{GeV}/c^2$.

the resonance claims.

One of the first experiments of photoproduction of $p\bar{p}$ pairs in the $\gamma p \to pp\bar{p}$ reaction was conducted at DESY in 1983 [9]. They observed two resonances with masses of $1.936\,\mathrm{GeV}/c^2$ and $2.024\,\mathrm{GeV}/c^2$, respectively, with 230 measured events (see Fig. 1). Also, there have been several analyses of the reaction $\bar{p}p \to \bar{p}p\pi^+\pi^-$ measured at CERN which either observed or deny the existence of a $p\bar{p}$ resonance at around $2\,\mathrm{GeV}/c^2$ [6, 10]. In these analyses, the observation of a resonance depends on the choice of kinematic cuts, that would enhance favorably resonance production mechanism.

Since the beginning of the new millennium there have been analyses searching for baryon-antibaryon resonances in photoproduction with CLAS at Jefferson Lab and in radiative decays of J/ψ at BESIII [11, 12]. The first analysis of CLAS6 data utilized the g6b dataset which yield in total approximately 2,000 $p\bar{p}$ events [13] for beam energies from near-threshold

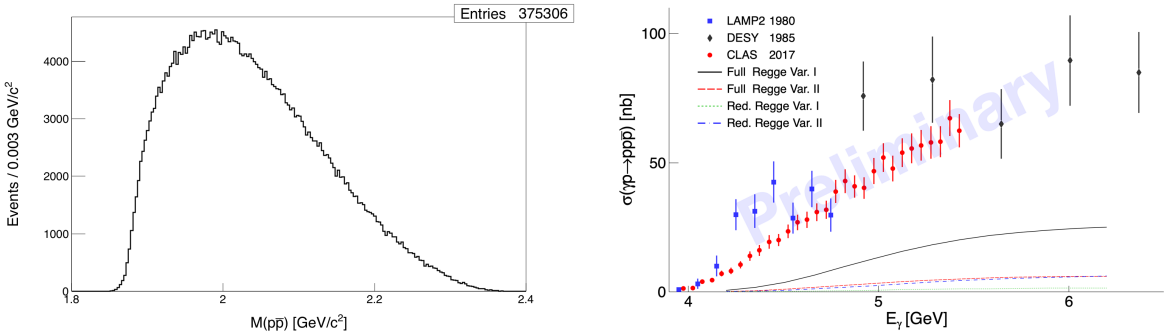

FIG. 2: Preliminary results from the photoproduction reaction $\gamma p \to pp\bar{p}$ from CLAS g12 data [15]: (left) The invariant mass distribution for $p\bar{p}$ where no resonance structure is visible and (right) the cross section as a function of photon beam energy (red points) compared to world data (LAMP2 [16] and DESY [9]). Various theoretical models from [17] underpredict the data.

to 5.3 GeV. The obtained $p_{\text{slow}}\bar{p}$ invariant mass spectrum suggested there may be hints of peaks, however a follow-up analysis using CLAS g6c data, which had about an order of magnitude larger statistics, did not observe any peaks [14]). The beam energies in g6c covered 4.8 to 5.5 GeV. The mass resolution was $\sim 3\,\text{MeV}/c^2$, thus, sufficient to observe resonances with widths of $20 - 40\,\text{MeV}/c^2$.

So far, the largest data set (200,000 events) for proton-antiproton photoproduction has been obtained with CLAS6 during the g12 experiment where a tagged real-photon beam with energy between 3.95 and 5.45 GeV was incident on a proton target [15]. The analysis of this data set did not show any resonance peaks. There was also no resonance observed in the $p\bar{p}$ invariant mass spectrum independently if the data were binned in or integrated over photon energies (see Fig. 2 (left)).

The main problem with the $\gamma p \to pp\bar{p}$ channel is the ambiguity from the two final state protons. In the previous analyses the protons are distinguished by their momenta and a fast and slow proton is determined for each event. This separation is also used to differentiate between reaction mechanisms (meson and baryon exchange, see Section II A 2). However, this discrimination is not perfect, thus, the ambiguity could hinder an observation of a resonance.

The reactions $\gamma n \to np\bar{p}$ and $\gamma d \to dp\bar{p}$ are free from ambiguities in the determination

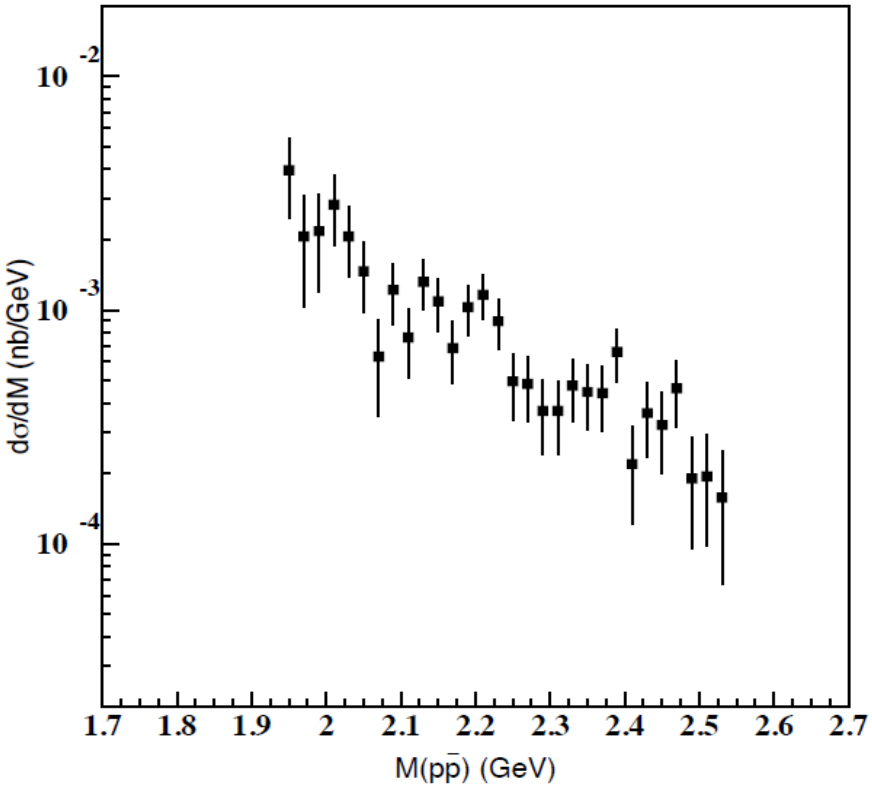

FIG. 3: The invariant mass distribution for $p\bar{p}$ in the coherent reaction $\gamma d \to dp\bar{p}$ from CLAS eg3 thesis [18]. Only about 300 events have been measured.

of the produced $p\bar{p}$ pair. The coherent $p\bar{p}$ production in $\gamma d \to dp\bar{p}$ has been studied with CLAS eg3 data [18]. The beam energy was up to 5.5 GeV and about 300 events survived the data selection cuts. The resulting $p\bar{p}$ spectrum is shown in Fig. 3. No resonances or peaks have been observed with such limited statistics. The $\gamma n \to np\bar{p}$ was not studied since the lower detection efficiency of the neutron compared to the deuteron would decrease the statistics further. There is no other measurement of this channel so far. A measurement of $p\bar{p}$ production on deuterium in CLAS12 during the remaining RG-B beam time would give comparable statistics to g12 data on a neutron target. We also expect to increase the statistics for the coherent deuteron production by a factor of 10.

2. Theoretical Description

Several theoretical models have been developed to describe possible narrow $p\bar{p}$ resonances [1–3]. It was hypothesized that if the resonances prefer to decay into a baryon-antibaryon

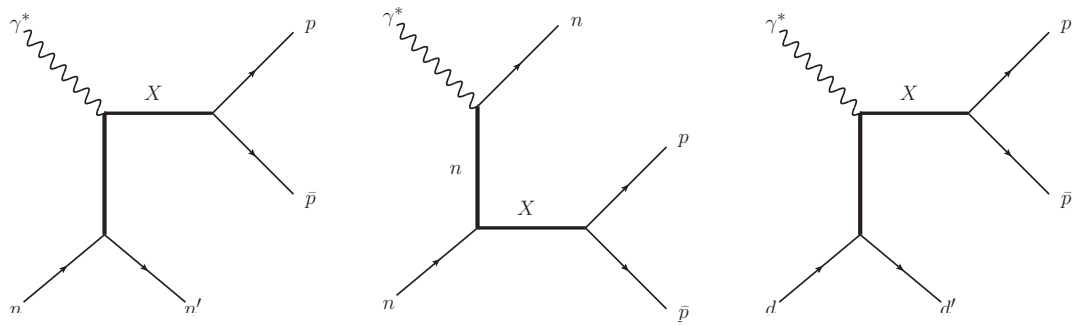

(a) $\gamma n \to np\bar{p}$ (b) $\gamma n \to np\bar{p}$ (c) $\gamma d \to dp\bar{p}$

FIG. 4: Main Feynman diagrams for resonance $p\bar{p}$ photoproduction off the neutron: (a) meson exchange (t-channel) and (b) baryon exchange (u-channel). The coherent production off the deuteron (c) is predominantly t-channel due to the deuteron form factor that suppresses large momentum transfer region in the u-channel.

final state instead of into mesons, they are not $q\bar{q}$ type resonances. Indeed, the most common hypotheses are describing such a resonance as a baryon-antibaryon state bound by nuclear forces or as a $(qq - \bar{q}\bar{q})$ state. There are also recent calculations which suggest that the resonances can in particular be glueballs [17]. All of the theoretical calculations heavily underestimate the measured differential cross section of the $\gamma p \to pp\bar{p}$ reaction [15] as shown in Fig. 2 (right). Note also, that even if the theoretical curves are scaled, they do not match to the data. This hints to either a significant contributions of an exotic production mechanism or the need to implement other meson states in the diagrams.

The production of a $p\bar{p}$ resonance could be via meson exchange (t-channel diagram) or baryon exchange (u-channel diagram). The basic diagrams for the neutron and deuteron are shown in Fig. 4. The t-channel mechanism dominates coherent production on the deuteron largely due to deuteron form-factor that suppresses large momentum transfer region.

In a previous analysis of $\gamma p \to pp\bar{p}$, it was found that the t-channel diagram dominates the $p\bar{p}$ production by a factor of 3 compared to the u-channel [14]. This result was obtained by model-dependent simulations using an incoherent sum of the different production mechanism fitted to data. We want to study this further by comparing the production on the neutron and the deuteron where different diagrams contribute. Furthermore, the reactions do not have the ambiguities of two protons in the final state which allows a cleaner study of the production mechanism.

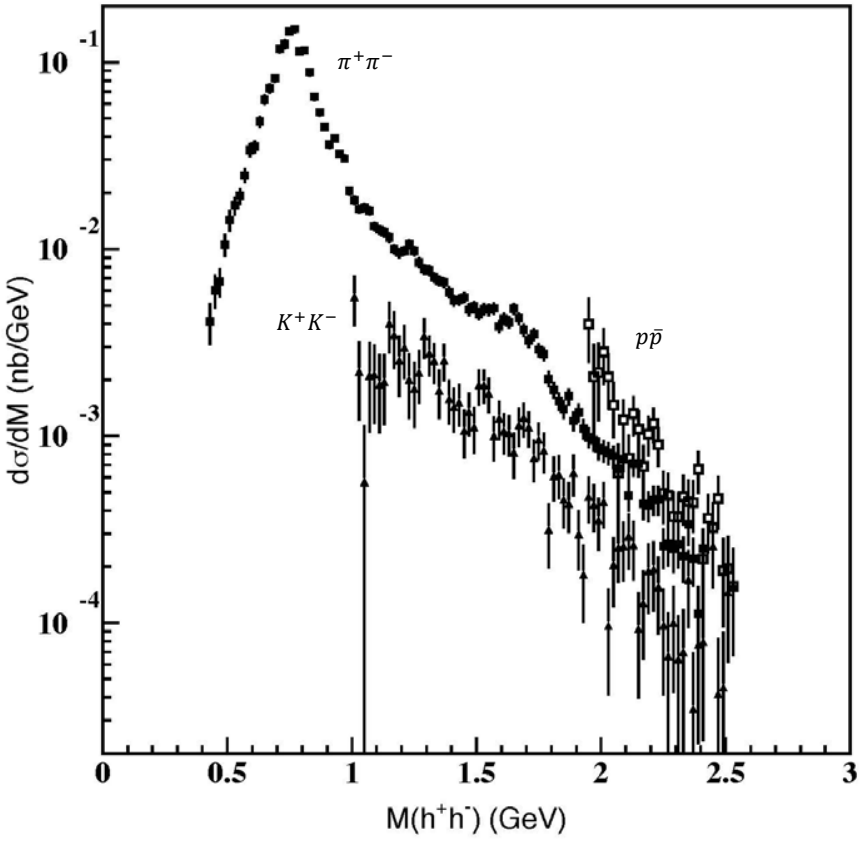

FIG. 5: The invariant mass distribution for $\pi^+\pi^-$, K^+K^- and $p\bar{p}$ in the coherent dihadron production reaction $\gamma d \to dh^+h^-$ from CLAS eg3 thesis [18]. For large invariant masses the $p\bar{p}$ cross section is larger than the $\pi^+\pi^-$ cross section.

B. Coherent Dihadron Production

We propose to study the coherent production of several types of dihadron pairs (without any other particle in the final state). In the previous CLAS6 analysis [18], this was studied for $\pi^+\pi^-$ and K^+K^- pairs beside $p\bar{p}$. The observed invariant mass spectra are shown in Fig. 5. The $p\bar{p}$ production rate is almost the same, even slightly higher, than the coherent production of $\pi^+\pi^-$ pairs. This is unexpected, since this indicates that t-channel photoproduction to 3-quarks and 3-antiquarks has the same rate as diffraction to two $q\bar{q}$ pairs. A similarly large yield was observed by the L3 collaboration [7] in $e^+e^- \to p\bar{p}$. This was explained by diquark-antidiquark production, $((qq)$-$(\bar{q}\bar{q}))$, in the model calculations [19, 20].

Diquarks are not color neutral and, therefore, do not exist as free bound states. While

there properties and dynamics are highly disputed, diquarks have been used to explain the formation of baryonium and mesonlike states, e.g., $X(3872)$ [21]. Many spin effects observed in high-energy exclusive reactions pose severe problems for the pure quark picture of baryons and might be explained by the introduction of diquarks as hadronic constituents [22–24].

We propose to study the coherent production of $\pi^+\pi^-$, K^+K^- and $p\bar{p}$ pairs and extend with much larger statistics the previous measurement. Furthermore, invariant masses up to $3.5\,\mathrm{GeV}/c^2$ will be covered which were not measured before. The obtained cross sections allow to understand the production mechanism by comparison to future theoretical calculations.

III. PROPOSED MEASUREMENT

The proposed measurement aims to study the $p\bar{p}$ photoproduction on a neutron and the coherent dihadron production on a deuteron. A deuterium target will be used as an effective neutron target. The quasi-real photons will be produced by the incident electron beam in the target. We want to collect data with tagged and untagged photoproduction and determine the invariant dihadron spectra ($d\sigma/dm$) as well as the t-dependence of the cross section. We will look for resonances in the $p\bar{p}$ spectrum and study the coherent production mechanism by measuring the invariant dihadron spectra of pion, kaon and $p\bar{p}$ pairs on a deuteron.

The measurement will be performed in HallB using the CLAS12 detector and the CLAS12 Forward Tagger (FT). CLAS12 consists of the forward detector (FD) and the central detector (CD) [25]. The forward detector is able to detect and identify charged and neutral particles scattered between 5° and 35° over the full momentum range. The particles are detected in six identical sectors within a sixfold superconducting toroidal magnet. Each sector is equipped with a set of drift chambers for tracking, a high-threshold Cherenkov counter (HTCC), the Low Threshold Cherenkov Counters (LTCC), scintillation counters (FTOF) for time-of-flight measurement, and a preshower (PCAL) and forward calorimeters (ECAL). The central detector consists of several layers of the central vertex tracker (CVT), the central time-of-flight scintillators (CTOF) and the central neutron detector (CND). The CLAS12 forward tagger consists of a scintillator hodoscope, a tracker and a lead-glass electromagnetic calorimeter and covers angles from 2.5° to 4.5°.

The charged hadrons will be detected and identified in the FD by utilizing the combination

of the tracking information from the DC and the particle identification of HTCC, LTCC and FTOF. The neutron and deuteron will be detected by time-of-flight and tracking either in the CND or the FD. For tagged photoproduction, the scattered electron will be detected by the Forward Tagger. This allows reconstruction of the neutron momentum distribution as a cross-check as well as the dependence of the observables on the beam energy.

To achieve larger statistics, we will not require the scattered electron to be detected in the FT (untagged photoproduction). The reaction can clearly be identified and reconstructed by the final state particles if all of them are detected by the forward and central detectors. In this scenario the t-distribution can be reconstructed by assuming that the incoming beam energy corresponds to the longitudinal momentum of the sum of the three final state particles where this method can be verified using tagged events. This assumption is completely valid for the deuteron in the coherent production but an approximation in the neutron case due to the Fermi momentum. Nevertheless, the Fermi momentum is small compared to the energy of the incoming photon beam.

The experimental setup for our proposal would be the same as for run-group B (RG-B) during the beam time in Spring 2019. The only necessary modification is a change in one of the existing triggers which will be explained in the Section IV A. We are not requesting extra beamtime that was not already allocated to RG-B. Therefore, our rate predictions are based on the total approved 90 PAC days subtracted by the Spring 2019 beam (21 PAC days[1]) time which gives 69 remaining PAC days. The estimates of the luminosity and achievable statistics shown in Section V and IV C are based on these number of days.

We prefer to have an electron beam energy of 11 GeV for this proposal. However, the invariant mass region where $p\bar{p}$ resonances have been observed previously is also covered with lower beam energies[2].

IV. TRIGGER SETUP AND LUMINOSITIES

In this section the necessary trigger conditions for the measurement in this proposal are described. Furthermore, the electron luminosity and photon flux in the remaining RG-B approved beam time is estimated.

[1] This number was reported by RG-B for 4 of their 7 experiments taking into account the change of beam energy in Spring 2019. However, other experiments of RG-B reported less effective time due to the change in beam energy.

[2] The beam energy in Fall 2019 will be between 10.2 to 10.6 GeV. All of these beam energies are acceptable.

A. Trigger Requirements and Rates

To determine the trigger conditions for our proposed measurement, we simulated the reactions $\gamma n \to np\bar{p}$ and $\gamma d \to dp\bar{p}$ with the CLAS12 fast Monte Carlo simulation. We generated the beam photons according to the bremsstrahlung spectrum for an electron beam of 11 GeV and the event distributions according to two-body phase space weighted by a t-slope of $3\,(\mathrm{GeV}/c)^{-2}$. The proton and antiproton in the simulation are predominantly in opposite sectors independently on the reaction, on cuts on generated $p\bar{p}$ mass and on the generated photon energies (see Fig. 6). Therefore, we are proposing to use a trigger with two forward going hadrons with opposite charge and opposite sector ($\Delta\phi \approx 180°$).

A similar trigger was already used during the Spring 2019 beam time of RG-B. This trigger demands two opposite-charged tracks in the drift chambers with coincident hits in the FTOF and PCAL/ECAL. Furthermore, the tracks have to be in opposite sectors and the energy deposition cut in the electromagnetic calorimeter (ECAL) has to below a maximum value (EMAX) for dimuon identification for the J/ψ measurements. The necessary trigger for our proposal would include this dimuon trigger completely, and, therefore, not affect the J/ψ experiment of RG-B. The experimental trigger rates during the RG-B run time in Spring 2019 are shown in Fig. 7 (bits 7-12). The total rate was about 8 kHz[3] at 50 nA beam current [26].

The CLAS12 DAQ system can handle a total rate of about 25 kHz [26, 27]. Fig. 7 shows that the trigger rate for electrons is about 6 kHz. Therefore, there is up to 19 kHz rate available for the proposed trigger without the maximum energy deposition cut in ECAL of the Forward Detector (FD).

We expect that the trigger for two tracks with opposite charges in two opposite sectors will be increased by 50 % when the maximum deposition cut in ECAL is removed from the current two-sector trigger. This is confirmed by measured rates shown for bits 14-19 in Fig. 7 which do not have the ECAL cut, which were observed during trigger studies in the spring 2019 RGB run. This rate will be about 12 kHz, giving a total trigger rate of 18 kHz (including the electron).

A summary of the expected trigger rates for the various RG-B trigger configurations,

[3] The total rate is not the sum of the rates for bits 7-12 since there is double counting in the single rates. [26]

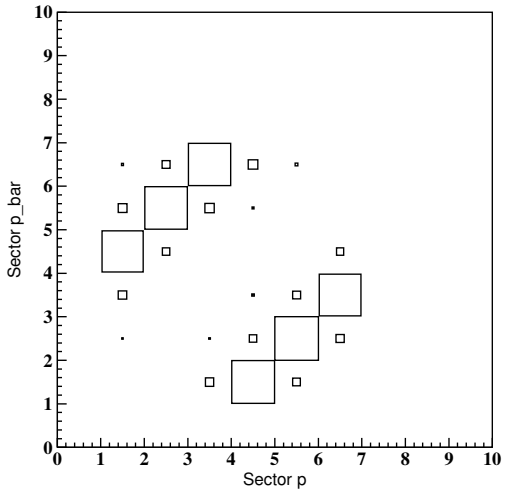

(a) $\gamma n \to np\bar{p}$ with generated $p\bar{p}$ mass limit $[2m_p, 3.0\,\mathrm{GeV}/c^2]$.

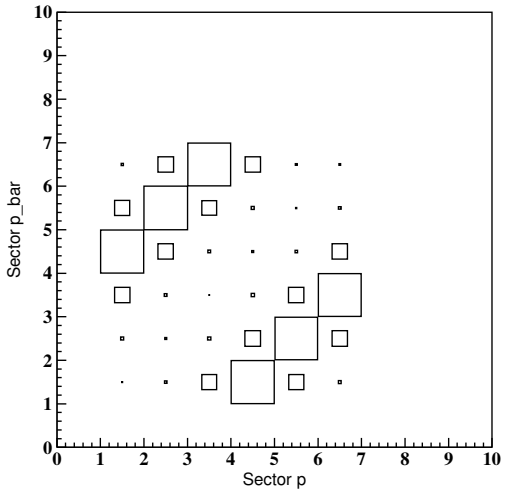

(b) $\gamma d \to dp\bar{p}$ with generated $p\bar{p}$ mass limit $[2m_p, 3.0\,\mathrm{GeV}/c^2]$.

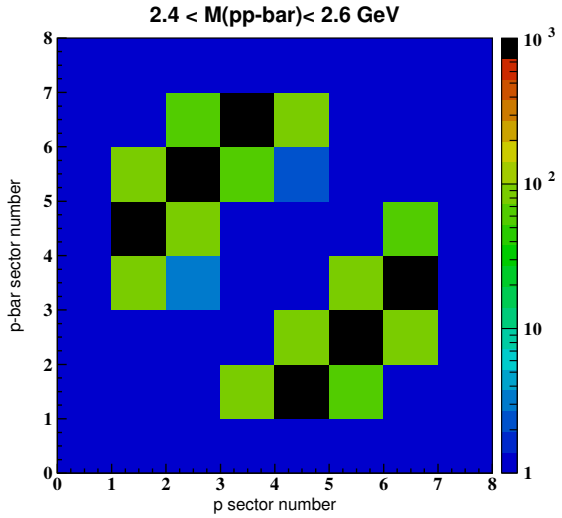

(c) $\gamma d \to dp\bar{p}$ with generated $p\bar{p}$ mass limit $[2.4\,\mathrm{GeV}/c^2, 2.6\,\mathrm{GeV}/c^2]$.

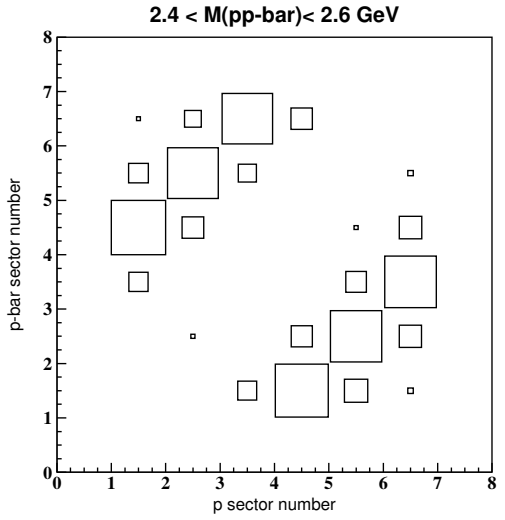

(d) $\gamma d \to dp\bar{p}$ with generated $p\bar{p}$ mass limit $[2.4\,\mathrm{GeV}/c^2, 2.6\,\mathrm{GeV}/c^2]$ and a photon beam limit from 7 to 9 GeV.

FIG. 6: Fast Monte Carlo results for $\gamma n \to np\bar{p}$ (a) and $\gamma d \to dp\bar{p}$ (b-d) showing that the proton and antiproton are scattered predominantly in opposite sectors for both reactions, independently of simulated invariant mass or beam energy ranges. All plots are obtained according to a cross section with a t-slope of $3\,(\mathrm{GeV}/c)^{-2}$. The lower two plots are only generated in a mass range of $[2.4\,\mathrm{GeV}/c^2, 2.6\,\mathrm{GeV}/c^2]$ with an extra limit on generated beam energy from 7 to 9 GeV for the lower right (d) plot.

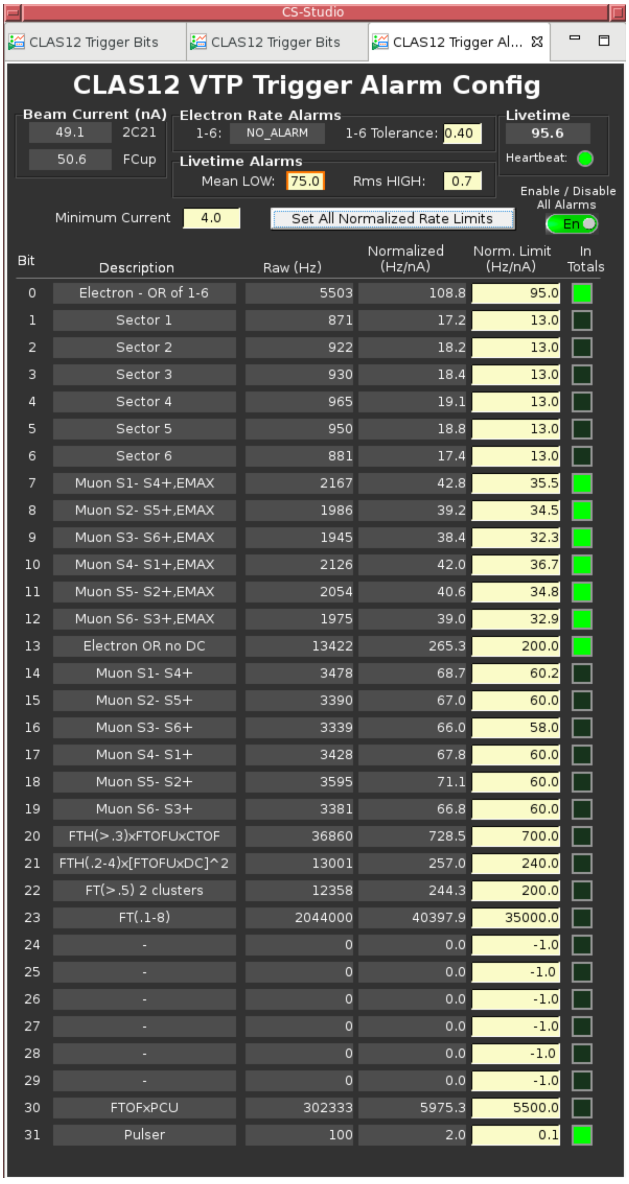

FIG. 7: RG-B trigger rates with a 50 nA beam on deuterium target as measured in Spring 2019. Trigger bits $14-19$ count the two-particle, opposite-sector and opposite-charge triggers without a maximum energy deposition cut in the electromagnetic calorimeter, while bits $7-12$ show the rate with the cut. The label of each of these trigger bits denote the combination of sectors in the Forward Detectors.

including the proposed one, is given in Table I.

Trigger	Rate [kHz]
Maximum DAQ rate	25
2 Hadrons opposite-sector, opposite-charge and EMAX cut (J/ψ trigger during RG-B)	8
2 Hadrons opposite-sector and opposite-charge	12
Electrons in Forward Detector	6
Total rate with proposed trigger configuration	18

TABLE I: Expected trigger rates for RG-B at 50 nA beam current. EMAX is a cut on the energy deposition in the electronmagnetic calorimeter (ECAL) of CLAS12. The values are obtained from the Spring 2019 data and trigger tests done at that time.

B. Photon Flux Estimate

Here, we want to estimate the photon flux for the untagged and tagged photoproduction cases. When the photon is not tagged i.e. the scattered electron is not detected by the Forward Tagger, the total flux of photons is the sum of the virtual photon flux and the real photon flux produced from bremsstrahlung of the electrons in the target. As shown by previous proposals and notes [28–30], the virtual photon flux is about a factor 2 larger than the flux from bremsstrahlung (we also verified this by using Eq. (5) of [30] and integrating over the photon energies). Therefore, for the rate estimates we are using a calculated flux from bremsstrahlung as a conservative estimate of the luminosity. Specifically, the number of photons per electron is given by the standard formula [31]:

$$n(E_\gamma) = \int_{E_\gamma^{\min}}^{E_\gamma^{\max}} \frac{d}{2 \cdot \chi_0} \left(\frac{4}{3E_\gamma} - \frac{4}{3E_b} + \frac{E_\gamma}{E_b^2} \right) \mathrm{d}E_\gamma, \tag{1}$$

where E_b is the electron beam energy, $d = l \cdot \rho$ is the target areal density and χ_0 is the radiation length of the target material. For the RG-B deuterium target the values are $d = 5\,\mathrm{cm} \cdot 0.163\,\mathrm{g/cm^3} = 0.815\,\mathrm{g/cm^2}$ and $\chi_0 = 126\,\mathrm{g/cm^2}$. Using $E_\gamma^{\min} = 6\,\mathrm{GeV}$ and $E_\gamma^{\max} = 10.6\,\mathrm{GeV}$[4], we get $n(E_\gamma) = 2.3 \cdot 10^{-3}$ per electron.

[4] It is still unclear if the beam energy will be 10.2 or 10.6 GeV in Fall 2019. For our calculations we use the optimistic value of 10.6 GeV. The luminosity would only be 3-4 % less for the lower beam energy.

C. Luminosities

The expected luminosity for the untagged photon beam for the remaining approved 69 PAC days of RG-B is calculated from the electron luminosity. We expect to run at 50 nA beam current as in spring 2019 which gives an integrated charge of 300 mC. Given the target density and length from above, the integrated electron luminosity will be $\mathcal{L}_e = 450\,\mathrm{fb}^{-1}$. This gives an untagged photon luminosity of $\mathcal{L}_{\gamma,\mathrm{untagged}} = \mathcal{L}_e \cdot n(E_\gamma) = 1\,\mathrm{fb}^{-1}$.

To obtain the flux for tagged photoproduction, the angular acceptance of the Forward Tagger has to be considered. i.e $2.5^\circ < \theta_{e'} < 4.5^\circ$. From previous calculation [29], we know that this gives about an order of magnitude lower luminosity than untagged production. Thus, we estimate the tagged photon luminosity to be $\mathcal{L}_{\gamma,\mathrm{tagged}} = 100\,\mathrm{pb}^{-1}$. This value is again a conservative estimate since we were already using a lower limit for the calculation of the untagged photoproduction luminosity.

V. DATA RATES AND DISTRIBUTIONS

From the known photon luminosity we can now estimate the rates and study distributions for the reactions $\gamma n \to np\bar{p}$ and coherent production of $p\bar{p}$, $\pi^+\pi^-$ and K^+K^- in γd.

We determine the acceptances to detect the final-state particles with inbending field of the CLAS torus magnet by simulations with GEMC 4.3.0 [32] and reconstruction with coatjava version 5.9.0. The simulation was using a two-body phase space generator developed for the g12 analysis [15]. The reaction is generated with a bremsstrahlung photon spectrum between 6.5 and 10.5 GeV and a t-channel model with a slope of $1.5\,(\mathrm{GeV}/c)^{-2}$. The $p\bar{p}$ system decays as two-body phase space. All estimations are for the remaining approved RG-B beam time. We are expecting to collect 1/3 of the data during the scheduled RG-B beam time in Fall 2019.

A. $\gamma n \to np\bar{p}$ Statistics and Distributions

The estimation of the cross section for the $\gamma n \to np\bar{p}$ reaction at our energy regime was done by extrapolating from the unpublished cross section measurements of CLAS6 for $\gamma p \to pp\bar{p}$ up to a beam energy of 5.45 GeV. The result of this measurement is shown in Fig. 2 (right). One can see that the cross section increases with photon energies. We are

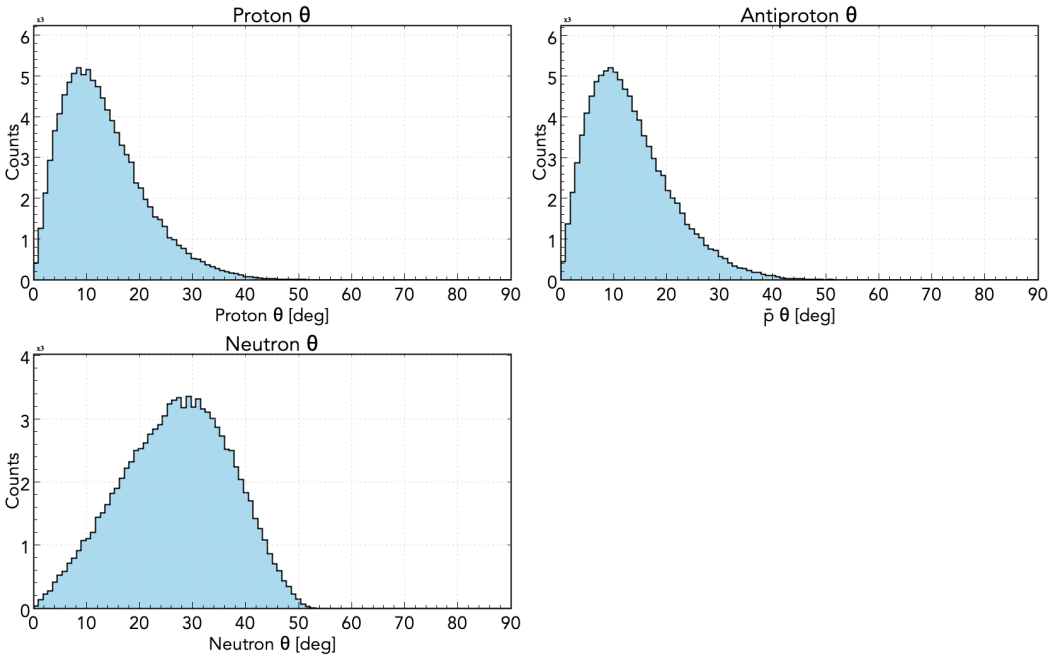

FIG. 8: Generated angular distributions of the final state particles in $\gamma n \to np\bar{p}$ using a two-body phase-space generator with a bremsstrahlung photon spectrum from 6.5 GeV to 10.5 GeV and a t-channel model with a slope of 1.5 $(\mathrm{GeV}/c)^{-2}$. The plots illustrate the expected range of the scattering polar angle of the three particles. As expected, the proton and antiproton are going predominantly into the FD of CLAS12.

expecting that this will continue for larger photon energies. Therefore, we are using 50 nb for our estimations as a conservative lower limit of the cross section in the energy region of interest. From the GEMC simulation we obtained a value of 1.6 % for the combined detection efficiency and geometrical acceptance. Combining the cross section with efficiency, acceptance and luminosity gives a total of $7.5 \cdot 10^5$ events for the untagged photoproduction. This is larger than the statistics obtained on a proton target from the CLAS6 g12 data. We expect already $2.5 \cdot 10^5$ events this fall. In case of a tagged photon in the Forward Tagger the rate will drop by an order of magnitude which would still give a compatible data sample to g12 and g6c.

Fig. 8 shows the angular distributions of the neutron, proton and antiproton in the lab frame from the GEMC simulations. From the generated values shown, one can see that the proton and antiproton are going predominantly into the Forward Detector which has a coverage from about 8° till 35° for negative charged particles and 5° till 35° for positive

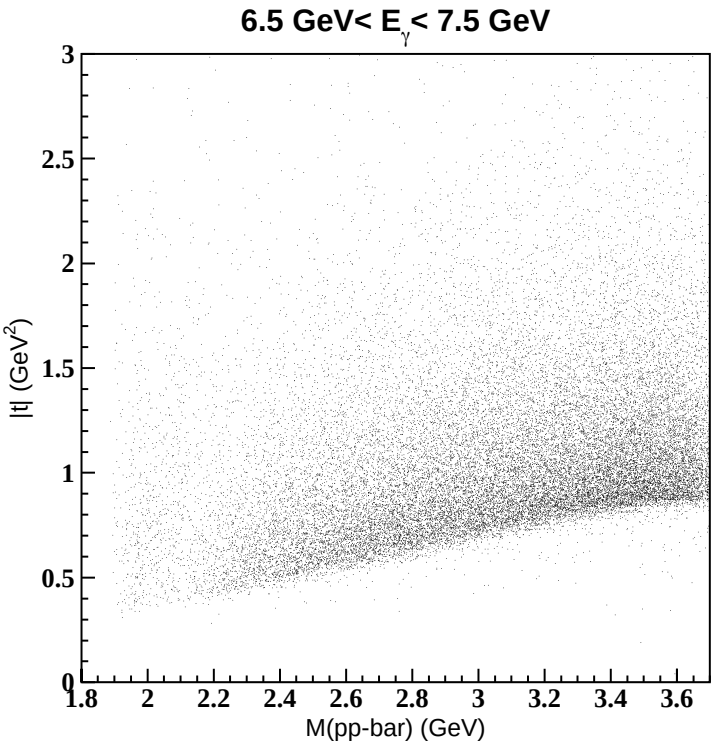

FIG. 9: t versus $m_{p\bar{p}}$ distribution for photon energies between 6.5 and 7.5 GeV of the $\gamma n \to np\bar{p}$ from the fast MC simulations used to determine the trigger condition. It shows the typical coverage in momentum transfer, t, and invariant mass $m_{p\bar{p}}$ for our data as well as the dependence of t_{min} on the invariant mass.

charged particles with full inbending field of the torus magnet. As already shown in Section IV A, the proton and antiproton have usually an azimuthal angle difference of 180° hence they are going into opposite sectors of CLAS. The neutron will be detected either in the calorimeters in the Forward Detectors or in the Central Neutron Detector for neutrons with larger angle.

In Fig. 9 the coverage for t versus the $p\bar{p}$ invariant mass is shown for beam photon energies between 6.5 and 7.5 GeV obtained from the fast MC simulations used to study the trigger conditions for this proposal (see Fig. 6). In previous measurements only invariant masses up to 2.4 GeV/c^2 were covered. The visible ridge at low momentum transfer is the kinematical limit which depends on the invariant mass.

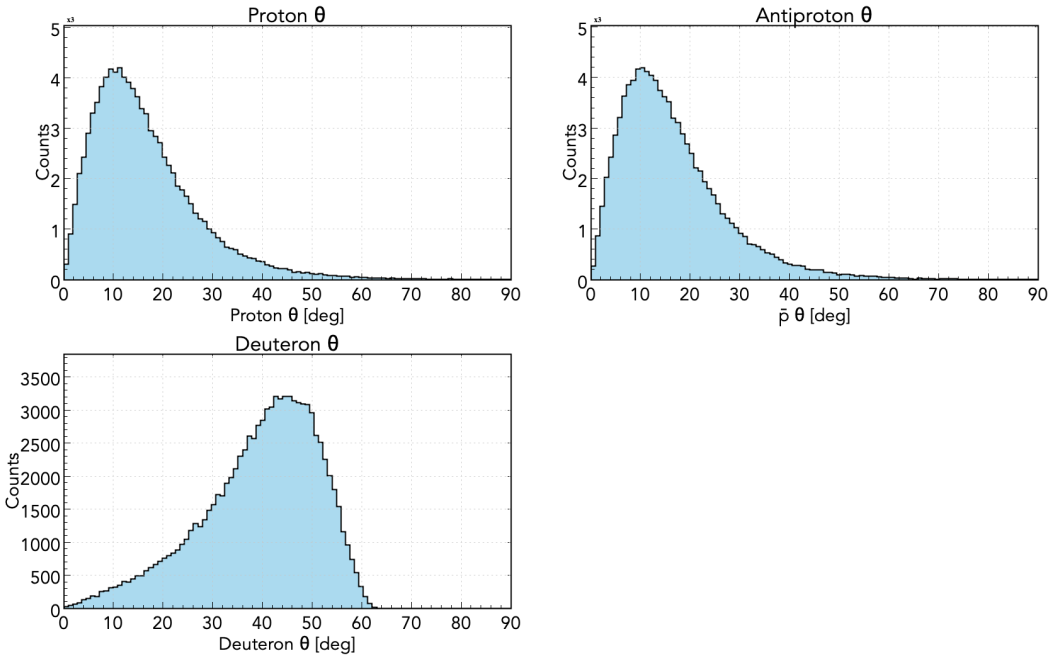

FIG. 10: Generated angular distributions of the final state particles in $\gamma d \to dp\bar{p}$using a two-body phase-space generator with $p\bar{p}$ as a pseudo particle. A photon energy range from 6.5 GeV to 10.5 GeV and a t-slope of 1.5 $(\mathrm{GeV}/c)^{-2}$ were used. The plots illustrate the expected range of the scattering polar angle of the three particles. As expected, the proton and antiproton are going predominantly into the FD of CLAS12.

B. $\gamma d \to dp\bar{p}$ Statistics and Distributions

For the coherent production we estimated our event rate from the eg3 measurement. Their luminosity was 15 pb^{-1} taking into account some trigger inefficiencies [33] which gave 2400 after dividing through the acceptance. Assuming the same cross section for our beam energy, we expect $1.6 \cdot 10^5$ events without taking into account acceptances and efficiencies for 1 fb^{-1} luminosity. Our detection efficiency and acceptance for the three particle final-state $dp\bar{p}$ was obtained from simulations to be 2 %. Therefore, about 3300 events are produced for the untagged photoproduction which is by about a factor 10 larger than in the eg3 measurement. We expect already 1100 events in the beamtime Fall 2019.

Fig. 10 shows the angular distributions of the deuteron, proton and antiproton in the lab frame from GEMC simulations. The simulation was using a two-body phase space generator developed for the g12 analysis [15]. The reaction is generated with a bremsstrahlung photon spectrum between 6.5 and 10.5 GeV and a t-channel model with a slope of 1.5 $(\mathrm{GeV}/c)^{-2}$

[18]. The $p\bar{p}$ system decays as two-body phase space. From the generated values shown, one can see that the proton and antiproton are going predominantly into the Forward Detector which has a coverage from about 8° till 35° for negative charged particles and 5° till 35° for positive charged particles with full inbending field of the torus magnet. As already shown in Section IV A, the proton and antiproton have usually an azimuthal angle difference of 180° hence they are going into opposite sectors of CLAS. The deuteron will go mainly into the central detector of CLAS12 compared to $\gamma n \to np\bar{p}$. This is expected since the deuteron is heavier than the neutron hence less forward boost.

C. Yield for Coherent Production of $\pi^+\pi^-$ and K^+K^-

For the coherent production of $\pi^+\pi^-$ and K^+K^- pairs, the statistics will be dominated by pairs with invariant masses lower than $m_{p\bar{p}} = 2m_p$ due to the larger cross section i.e. $\pi^+\pi^-$ pairs from ρ production (see Fig. 5). Here, we only want to estimate the number of pion and kaon pairs for the $p\bar{p}$ invariant mass range from the obtained rates for proton-antiproton production since the t-dependence in this range was the same [18]. According to the previous measurement in [18], the rate of $\pi^+\pi^-$ is a factor of 1.5 less than $p\bar{p}$ for masses larger than $1.9\,\mathrm{GeV}/c^2$ while the rate of K^+K^- pairs is a factor 6 less. Therefore, we expect about 2200 $\pi^+\pi^-$ pairs and 500 K^+K^- for 69 PAC days.

D. Invariant Mass Resolution

For the detection of $p\bar{p}$ resonances, it is crucial to have a good invariant mass resolution. We studied the CLAS12 $p\bar{p}$ resolution by generating $\gamma n \to np\bar{p}$ two-body phase space events with fix $m_{p\bar{p}}$ masses. The t-slope and photon energy range are the same as before for the acceptance study (see Section V A). The generated events are then reconstructed by coatjava and the resulting invariant mass spectrum is fit with a Gaussian to obtain the resolution. In Fig. 11, the reconstructed invariant mass spectrum is shown for generated masses of $2.0\,\mathrm{GeV}/c^2$ (top left), $2.1\,\mathrm{GeV}/c^2$ (top middle), $2.2\,\mathrm{GeV}/c^2$ (top right), $2.3\,\mathrm{GeV}/c^2$ (bottom left) and $2.4\,\mathrm{GeV}/c^2$ (bottom right). One can see that the resolutions are between $2\,\mathrm{MeV}/c^2$ to $4\,\mathrm{MeV}/c^2$ similar to the CLAS6 resolution of the previous experiments on proton-antiproton photoproduction. This resolution is sufficient to detect $p\bar{p}$ resonances

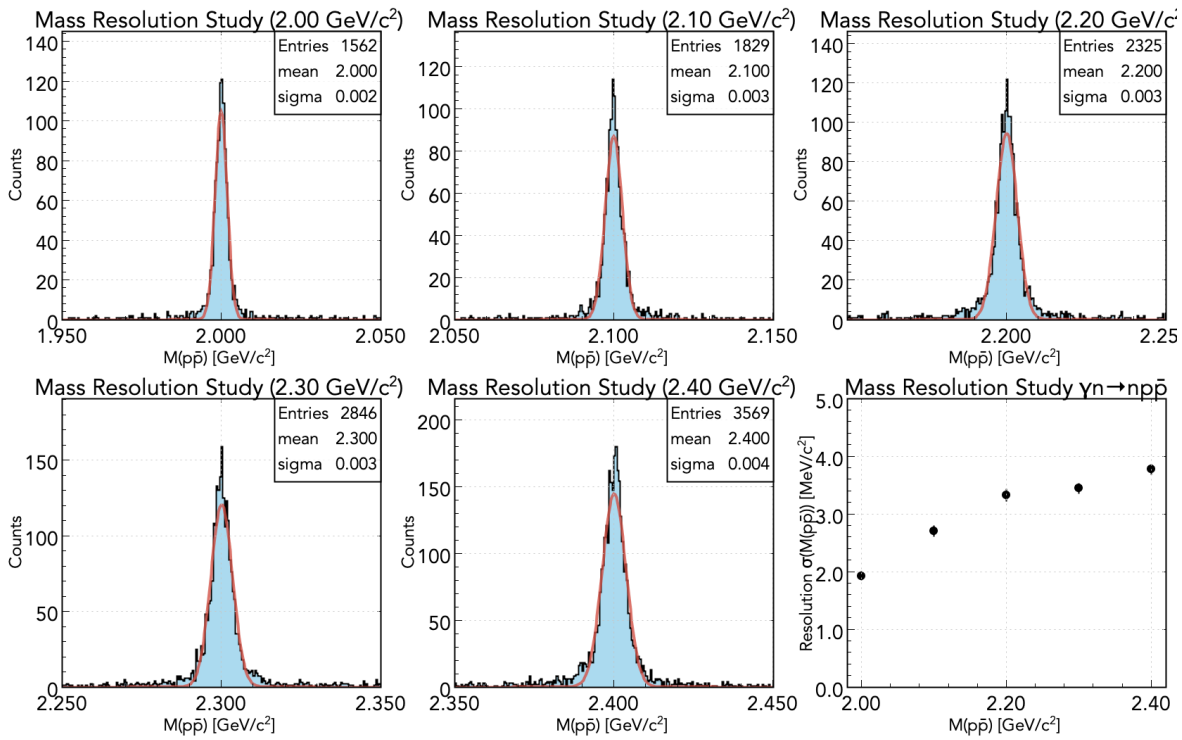

FIG. 11: Reconstructed $p\bar{p}$ invariant mass for 200,000 simulated events of $\gamma n \to np\bar{p}$ with a fixed $p\bar{p}$ mass of $2.0\,\mathrm{GeV}/c^2$ (top left), $2.1\,\mathrm{GeV}/c^2$ (top middle), $2.2\,\mathrm{GeV}/c^2$ (top right), $2.3\,\mathrm{GeV}/c^2$ (bottom left) and $2.4\,\mathrm{GeV}/c^2$ (bottom right). From a Gaussian fit, we obtain the resolution for each simulation. The values are between $2\,\mathrm{MeV}/c^2$ to $4\,\mathrm{MeV}/c^2$ which are shown as a function of simulated invariant mass in the bottom right plot.

with width of $20\,\mathrm{MeV}/c^2$.

VI. SUMMARY AND REQUEST

In summary, we are proposing to measure the photoproduction of $p\bar{p}$ off the neutron and coherently off the deuteron to search for narrow $p\bar{p}$ resonances in the invariant mass distribution, $d\sigma/dm$, and to understand the production mechanism of $p\bar{p}$. The coverage in $p\bar{p}$ invariant mass and momentum transfer t is extended to yet unmeasured regions. The comparison with the production of $\pi^+\pi^-$ and K^+K^- pairs off deuteron allows to understand the diffractive production mechanism, e.g., production via a diquark pair, qq and $\bar{q}\bar{q}$, instead of $(q\bar{q})$ pairs. Previous experiments indicated a much larger $dp\bar{p}$ cross section than expected which could be due to $qq - \bar{q}\bar{q}$ production [7, 18].

		Note
PAC days	69	RG-B beam time without spring 2019
Energy	11 GeV	Could be also slightly lower (see text)
Current	$\geq$ 50 nA	
Polarization	n/A	
Trigger	2 particles in FD	Opposite charge in opposite sector
Setup	CLAS12 and FT	Similar to spring 2019 setup
Torus field	full field, inbending	

TABLE II: Run days and experimental parameters for this proposal.

This measurement will be part of the remaining approved run group B beam time of CLAS12 which will be 69 PAC days. The maximum beam energy of 11 GeV is desired for this experiment to reach the highest photon energies, invariant masses and momentum transfers. However, a slightly lower beam energy of 10.2 GeV[5] does not effect the search for resonances significantly since the region where resonances have been observed in previous experiments (1.9 - 2.1 GeV/c^2) is well covered. We would only have a 5-10 % lower statistics from the reduced photon flux and a reduced kinematic coverage.

We do not require any degree of polarization of the beam and we are expecting to run with at least 50 nA beam current. This gives sufficient statistics within the 69 PAC days to achieve the scientific objectives of the proposal. The detector configuration needs to be similar to the one during the Spring 2019 RG-B beam time. That means an inbending, full torus field of CLAS12 and the operation of the Forward Tagger. The hadronic final-state particles will be measured by CLAS12 Forward and Central detectors while electrons from tagged photoproduction will be measured by the Forward Tagger.

For our proposed measurement, we need a two-particle opposite-sector and opposite-charge trigger in the Forward Detector of CLAS12. This trigger allows to record events of interest for the remaining RG-B beam time. It is an extension of the existing J/ψ dimuon trigger of RG-B, which uses in adddition a maximum energy deposit cut on ECAL. Our trigger will push the CLAS12 DAQ to 18 kHz for a beam current of 50 nA which is below the maximum acceptable rate [27].

[5] This was the lowest beam energy during the beam time of Spring 2019.

A summary of the conditions for this proposal is shown in Table II.

---

[1] H.-M. Chan and H. Hogaasen, Phys. Lett. **72B**, 400 (1978).

[2] M. Uehara, Prog. Theor. Phys. **61**, 1137 (1979).

[3] L. Montanet *et al.*, Phys. Rept. **63**, 149 (1980).

[4] P. Benkheiri *et al.*, Phys. Lett. **68B**, 483 (1977).

[5] B. G. Gibbard *et al.*, Phys. Rev. Lett. **42**, 1593 (1979).

[6] A. Buzzo *et al.* (JETSET), Z. Phys. **C76**, 475 (1997), arXiv:hep-ex/9801015 [hep-ex].

[7] P. Achard *et al.* (L3), Phys. Lett. **B571**, 11 (2003), arXiv:hep-ex/0306017 [hep-ex].

[8] S. U. Chung *et al.*, Phys. Rev. Lett. **45**, 1611 (1980).

[9] J. Bodenkamp *et al.*, Phys. Lett. **133B**, 275 (1983).

[10] A. Ferrer *et al.*, Eur. Phys. J. **C10**, 249 (1999).

[11] J. Z. Bai *et al.* (BES), Phys. Rev. Lett. **91**, 022001 (2003), arXiv:hep-ex/0303006 [hep-ex].

[12] M. Ablikim *et al.* (BESIII), Phys. Rev. Lett. **108**, 112003 (2012), arXiv:1112.0942 [hep-ex].

[13] V. Koubarovski *et al.*, CLAS Analysis Note **2001-001** (2001).

[14] B. Stokes, *Search for Resonances in the Photoproduction of Proton-Antiproton Pairs*, Ph.D. thesis, Florida International University (2006).

[15] W. Phelps, *Antibaryon Photoproduction using CLAS at Jefferson Lab*, Ph.D. thesis, Florida International University (2017).

[16] D. P. Barber *et al.*, Phys. Lett. **90B**, 470 (1980).

[17] T. Gutsche *et al.*, Phys. Rev. **D94**, 034010 (2016), arXiv:1605.01035 [hep-ph].

[18] Y. Ghandilyan, *Coherent Photoproduction of proton anti-proton pair on deuterium with CLAS*, Ph.D. thesis, A.I. Alikhanyan National Science Laboratory (Yerevan Physics Institute) (2016).

[19] C. F. Berger *et al.*, Fizika **B8**, 371 (1999), arXiv:hep-ph/9901338 [hep-ph].

[20] C. F. Berger and W. Schweiger, Eur. Phys. J. **C28**, 249 (2003), arXiv:hep-ph/0212066 [hep-ph].

[21] M. Padmanath, C. B. Lang, and S. Prelovsek, Phys. Rev. **D92**, 034501 (2015), arXiv:1503.03257 [hep-lat].

[22] I. C. Cloet and G. A. Miller, Phys. Rev. **C86**, 015208 (2012), arXiv:1204.4422 [nucl-th].

[23] T. Maji and D. Chakrabarti, Phys. Rev. **D94**, 094020 (2016), arXiv:1608.07776 [hep-ph].

[24] T. Maji and D. Chakrabarti, Phys. Rev. **D95**, 074009 (2017), arXiv:1702.04557 [hep-ph].

[25] "Clas12 technical design report," https://www.jlab.org/Hall-B/clas12_tdr.pd.

[26] V. Kubarovsky, "Private communication,".

[27] S. Boyarinov, "Private communication,".

[28] A. Afanasev *et al.*, "Photoproduction of the Very Strangest Baryons on a Proton Target in CLAS12," (2011).

[29] M. Battaglieri *et al.*, "Near threshold J/ψ photoproduction and study of LHCb pentaquarks with CLAS12," (2016).

[30] M. Battaglieri *et al.*, CLAS12 Analysis Note **2015-007** (2015).

[31] M. Tanabashi *et al.* (Particle Data Group), Phys. Rev. **D98**, 030001 (2018).

[32] GEMC, https://gemc.jlab.org/gemc/html/index.html.

[33] H. Egiyan *et al.*, CLAS Analysis Note **2009-104** (2009).